ORIGINAL ARTICLE

Non-destructive tests for performance evaluation of self-healing concrete by addition of methyl methacrylate-containing microcapsules

Ensaios não destrutivos para avaliação do desempenho de concreto autocicatrizante por adição de microcápsulas contendo metacrilato de metila

Daniel Valerio[a] iD
Juliana Ferreira Fernandes[b] iD
Marcos Massao Futai[b] iD
Antonio Domingues de Figueiredo[c] iD
Idalina Vieira Aoki[a] iD

[a]Universidade de São Paulo – USP, Departamento de Engenharia Química, São Paulo, SP, Brasil
[b]Universidade de São Paulo – USP, Departamento de Engenharia de Estruturas e Geotécnica, São Paulo, SP, Brasil
[c]Universidade de São Paulo – USP, Departamento de Engenharia de Construção Civil, São Paulo, SP, Brasil

Abstract: The objective of this work was to develop a chemical admixture to make concrete capable to heal its fissures autonomously and, consequently, mitigate the concrete's reinforcement corrosion due to the ingress of aggressive agents. For that, polymeric microcapsules built by a shell of urea-formaldehyde-melamine (UFM) and a core of methylmethacrylate were developed and added to the concrete to further evaluation. The concrete specimens containing 0%, 3% and 6% of the proposed microcapsules (mass of microcapsules / mass of cement) were subjected to destructive and non-destructive tests. The water absorption and the mechanical tests i.e., compressive strength and indirect tensile strength (Brazilian test) were carried out to characterize concrete, while the electrochemical impedance spectroscopy (EIS) and the non-destructive ultrasonic pulse velocity (UPV) tests were conducted to evaluate the concrete self-healing ability. These tests showed that the proposed admixture was able to heal the concrete's fissures partially. In addition, it was concluded that the samples with 3% of microcapsules presented higher self-repairing rates. Despite the microcapsules developed in this work have presented a satisfactory self-healing efficiency, their effectiveness looks to be affected by the mixing procedure once part of them is broken during the process.

Keywords: self-healing concrete, non-destructive tests, durability, fissures, corrosion.

Resumo O objetivo deste trabalho foi desenvolver um aditivo químico capaz de tornar o concreto auto reparável e, consequentemente, mitigar a corrosão da armadura em seu interior devido à entrada de agentes agressivos. Para isso, microcápsulas poliméricas compostas por uma casca de uréia-formaldeído-melamina (UFM) e um núcleo de metilmetacrilato foram desenvolvidas e adicionadas ao concreto para posterior avaliação. Os corpos de prova de concreto contendo 0%, 3% e 6% das microcápsulas propostas (massa de microcápsulas / massa de cimento) foram submetidos a ensaios destrutivos e não destrutivos. O ensaio de absorção de água e os mecânicos, ou seja, resistência à compressão e resistência à tração indireta (teste brasileiro) foram realizados para caracterizar o concreto, enquanto a espectroscopia de impedância eletroquímica (EIS) e os ensaios não destrutivos de velocidade de pulso ultrassônico (UPV) foram conduzidos para investigar a ocorrência de autorreparação. Esses testes mostraram que o aditivo proposto foi capaz de cicatrizar as fissuras do concreto parcialmente. Além disso, analisando os dados coletados com o programa de testes, concluiu-se que as amostras com 3% de microcápsulas apresentaram maiores taxas de autorreparação. Apesar das microcápsulas desenvolvidas neste trabalho terem apresentado uma eficiência de autorreparação

satisfatória, sua eficácia parece ser afetada pelo procedimento de mistura, uma vez que parte delas é quebrada durante o processo.

Palavras-chave: concreto auto cicatrizante, ensaios não destrutivos, durabilidade, fissuras, corrosão.

1 INTRODUCTION

Self-healing in polymeric materials was first reported in 2001 by the researcher Dr. Scott R. White from the Department of Aerospace Engineering at the University of Illinois [1]. After this, the interest in this topic has increased in the academic field. In 2005, the International Union of Laboratories and Experts in Construction Materials, Systems and Structures (RILEM) created the technical committee called Self-healing Phenomena in Cement-based Materials (221-SHC) to study self-healing phenomena in cement-based materials, with the aim of creating a concrete capable of repairing its own cracks.

Self-repair in concrete can be achieved through autogenous and autonomous mechanisms. The autogenous approach occurs due to the presence of particles similar in nature to concrete's components, such as fly ash, mineral crystallizing agents, or even cement in mixes with a low w/c ratio. Thus, when fissures are formed in concrete, and moisture can ingress in the cementitious matrix, the hydration of these particles generates products capable of repairing the damages. The former studies about autogenous self-healing in concrete began to appear from 1999 when autogenous healing was reported due to the hydration of non-hydrated cement particles and/or carbonation of calcium hydroxide [2], [3]. On the other hand, in the autonomous approach, self-healing agents of chemical or biological origin are encapsulated and incorporated into the concrete matrix. In those conditions, when the cracks appear, these agents are released and their action results in the partial or total filling of the fissures [4]-[6].

The self-healing concrete obtained by the autogenous approach has already been known for many years [7]. According to Zhenga et al. [8], concrete with crystallizing agents to promote self-repair is being successful used to build tunnels in China. In Brazil, the use of concrete mix designs with reduced w/c ratio, silica fume and crystallizing admixture were applied to large constructions in the Southeast region. As examples, it can be cited the tunnels in the region of the Port of Santos/Sao Paulo, the tunnel complex that is part of the Regis Bittencourt highway duplication at *Serra do Cafezal* in Sao Paulo, the overpressure slab of the Museum of Image and Sound (MIS) in Sao Paulo [9], and the fluid coverage of the Museum of Modern Art of Rio (M.A.R) [10], located in Rio de Janeiro. Images A and B in Figure 1 illustrate the last two works cited.
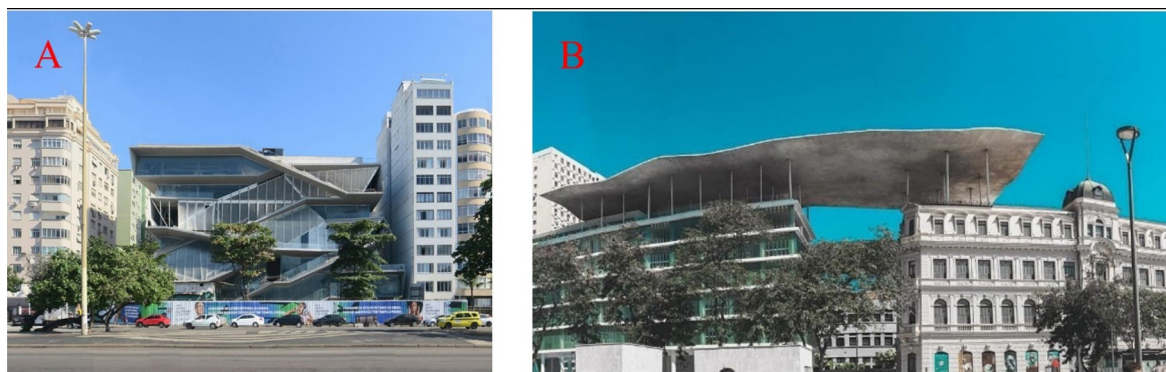
Figure 1. Constructions using self-healing concrete in Brazil: (a) Museum of Image and Sound in Sao Paulo [9]; (b) Museum of Modern Art of Rio (MAR) in Rio de Janeiro [10].

The autonomous self-healing in concrete has also been studied by several researchers [11]-[14]. In this type of approach, self-healing agents are entrapped in micro or nano capsules and added to the fresh concrete. The self-healing agents more commonly applied are bacterial spores as presented in the work developed by Jonkers et al. [15], and monomers as proposed by Tan et al. [16] and Yang et al. [17]. The autonomous self-healing is an attractive alternative due to three main reasons. First, it has a long activity once the self-healing agents are kept inside the microcapsules,

becoming active only when it is required/released. Second, it is easy to use once the microparticles can be added to a regular concrete mix design. Third, this sort of admixture has a low cost and easy synthesis.

The objectives of this work were to synthesize an admixture capable to provide self-healing properties to concrete and investigate the influence of this admixture on some concrete's properties, such as water absorption and mechanical strength. To achieve these aims the monomer methylmethacrylate (MMA) was doped with N, N-dimethyl-p-toluidine (DMPT) and entrapped in PUFM (polyurea-formaldehyde-melamine) polymeric microcapsules functionalized with the silane 3-Aminopropyltriethoxysilane (APTES), while the catalyst benzoyl peroxide (BPO) was added directly into the fresh concrete. In this context, when a fissure appears in the composite, the polymeric microcapsules are broken, the self-repairing monomer is released and flows through the cracks until it finds the catalyst that is dispersed in the concrete matrix. On the sequence the polymerization of the monomer begins, generating the polymer that occupies the region of the fissure, filling it up. The adoption of the proposed self-healing system was based on literature's analysis and previous experience on the encapsulation process [18], [19]. In addition, the decision was based on attractive aspects such as the low cost and availability of the raw materials (chemicals) used for synthesizing the microcapsules that makes up the self-repairing system.

2 MATERIALS AND EXPERIMENTAL PROGRAM

2.1 Materials

For the synthesis of PUFM microcapsules filled with the MMA and DMPT solution, the following materials were used: urea, resorcinol, arabic gum, sodium chloride, ammonium chloride, formaldehyde, hydrochloric acid, melamine, methylmethacrylate, and N, N dimethyl-p-toluidine.

For functionalizing the microcapsules, 3-aminopropyltriethoxysilane, ethyl alcohol, and distilled water were used.

All reagents used in this work had analytical grade purity.

For preparing reinforced concrete specimens, the following materials were used: CA – 50 carbon steel ribbed rebars with a diameter of 8.0 mm, stainless steel 316 L rebars with a diameter of 6.35 mm, cement CP II F 32 MPa, benzoyl peroxide, coarse aggregate with 9.5 mm of maximum size, medium size river sand as fine aggregate, and tap water.

2.2 Synthesis of the microcapsules

The PUFM microcapsules containing a solution of MMA and DMPT 1% (mass of MMA / mass of DMPT) functionalized with APTES, were obtained through an "in situ" emulsion polymerization process. The process was developed by Aoki and Cotting [18], and it is described in the deposited patent WO2014/032130 A1. The Figure 2 shows the microcapsules' synthesis scheme. After the production stage, the microcapsules were vacuum filtered, washed with distilled water and ethyl alcohol and, finally, functionalized.
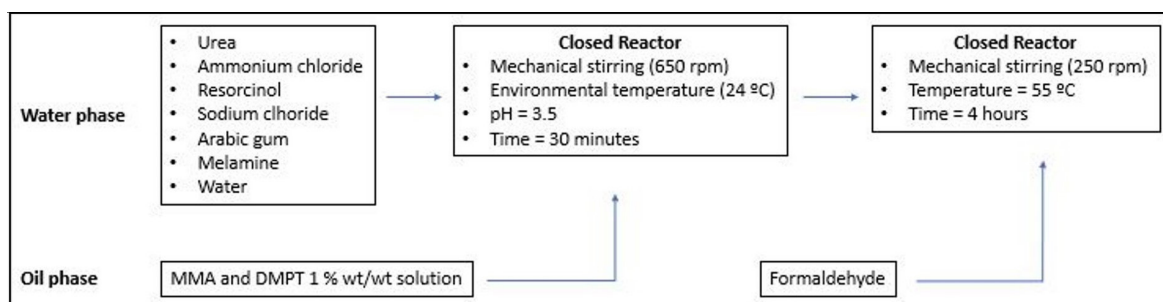
Figure 2. Scheme of the microcapsules' synthesis.

The functionalization routine consisted of placing the microcapsules in the hydrolyzed silane solution where they were left for 60 minutes under moderate agitation and a temperature of 40 °C. After this procedure, the microcapsules were washed with alcohol, vacuum filtered and stored in distilled water.

The hydrolyzed silane solution was prepared in two steps. First, equal volumes of distilled water and ethyl alcohol were mixed to be the solvent part of the hydrolysis. Second, the APTES was added (5% mass of APTES / mass of solvent). The solution was kept under moderate agitation and temperature of 40 ºC for 4 hours.

D. Valerio, J. F. Fernandes, M. M. Futai, A. D. Figueiredo, and I. V. AokiColarRunningAuthors

2.3 Techniques used for the microcapsule's characterization.

The microcapsules had their morphology and size distribution evaluated by means of Scanning Electronic Microscopy (SEM) and Laser Diffraction techniques, respectively. The equipment used to perform the analysis were a scanning electron microscope from Tescan, model Vega 3 LM and a laser diffraction particle size analyzer from Malvern, model Mastersizer 3000.

2.4 Specimen's production

To carry out the concrete properties and self-healing investigation tests, three types of specimens were cast. The Table 1 lists the specimen types and the tests they were submitted. The whole molding procedure was done in accordance with the Brazilian Association of Technical Standards ABNT NBR 5738 [20]. The images A, B, C, and D of Figure 3 illustrate each specimen type.

Table 1 - List of types of concrete specimens produced and the tests performed.

Type of specimens	Dimensions (mm)	Tests
Prismatic	170 x 100 x 100	Water absorption
Cubic	100 x 100 x 100	Ultrasound
Cylindrical	L = 200 e φ = 100	Mechanical characterization
Prismatic and reinforced	350 x 100 x 100	Electrochemical

As it can be seen in Figure 3D, the reinforced specimens were equipped with 3 steel rod bars. One central bar of stainless steel 316 L used as counter electrode (CE) and two side bars of carbon steel used as working electrodes (WE). The stainless-steel rebar had a contact area with the concrete equal to 64.8 cm^2, while each carbon steel rebar had a contact area equal to 50.26 cm^2. This difference in areas is necessary to make electrochemical tests feasible. The delimitation of the contact area of the carbon steel rebars with the concrete was made using the high-performance epoxy paint Interbond 998 PB. Figure 4 schematically illustrates the arrangement of steel rods in concrete specimens.

Figure 3. Illustration of the specimens: (A) prismatic; (B) cubic; (C) cylindrical; (D) Prismatics and reinforced.
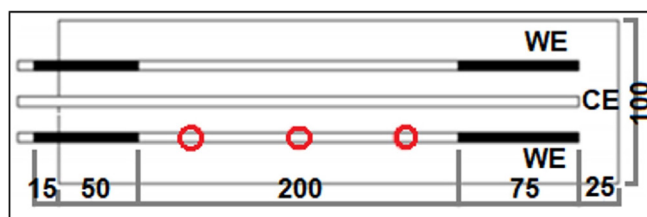
Figure 4. Schematic section of the lower longitudinal face of the prismatic and reinforced specimens. Dimensions in mm.

The concrete specimens were produced using a mix design that included 461 kg/m³ of CP II F 32 MPa cement, 922 kg/m³ of medium sand, 922 kg/m³ of crushed stone n° 0 and 299 kg/m³ of water. The specimens were all properly vibrated to ensure adequate compaction. The curing process was carried out in a humid chamber maintained at (23 ± 2) °C and 95% of relative humidity, for a period that varied between 80 and 90 days.

To cast the concrete specimens containing the self-healing system, the benzoyl peroxide (BPO) was added to the concrete mixer along with the other components of the concrete, in a proportion equal to 2% (mass of BPO / mass of microcapsules). The microcapsules were manually and carefully added into concrete while casting the specimens to ensure the lowest rate of prematurely broken particles. The dosages used in this work were 0%, 3% and 6% (mass of microcapsules / mass of cement).

For all the techniques used in this work, the samples without microcapsules (0% of admixtures) were called control, while the samples containing 3% and 6% of microcapsules were called ADT_3% and ADT_6%, respectively.

2.5 Methods for evaluating the influence of the proposed self-healing system on the characteristics of concrete

The absorption test and the determination of compressive and split tensile strengths (Brazilian test) were performed to investigate the influence of the proposed self-healing system on the inherent characteristics of concrete. The procedures used to the three aforementioned water evaluation techniques followed the methods established by the Brazilian Association of Technical Standards ABNT NBR 9778 [21], the ABNT NBR 5739 [22] and the ABNT NBR 7222 [23], respectively.

To carry the water absorption tests out, a drying oven of FANEM brand, model 315 SE, an analytical balance capable of made suspended weighing of OHAUS brand, model Adventurer ARD110, a Bunsen burner and a suitable container to leave the specimens in immersion were used.

The equipment used for the two mechanical characterization tests was a SHIMADZU universal servo-hydraulic testing machine, model UH – 2000kNXR which operates at a frequency of 60 Hz and has a load capacity of 2000 kN.

2.6 Self-healing activity verification

2.6.1 Ultrasonic Pulse Velocity Test (UPV)

The UPV technique can point out, in a comparative way, the existence of discontinuities such as fissures and cracks in concrete. The identification of discontinuities can be done either by checking the decrease in wave speed or the increase in the time the wave takes to travel through the concrete samples. The speed or travel time of the ultrasonic pulses vary because fissures and voids hinder the propagation of waves and, consequently, their arrival at the receiving transducer [24], [25].

To investigate the self-healing occurrence, UPV tests were performed at three different times: before, immediately after, and two days after intentionally fissuring the concrete specimens. Thus, it was possible to collect data from the same specimens in three different situations: intact, cracked, and self-healed, as 48 hours was established as the self-healing time.

The procedure for fissuring the cubic specimens in a controlled way was to apply 80% of the maximum compressive load. Similar procedures have been successfully used and reported by other authors [26], [27].

The UPV tests were performed in triplicate (three specimens from each group were analyzed) and following the guidelines established by the Brazilian Association of Technical Standards ABNT NBR 8802 [28]. For generating and reading the ultrasonic pulses, a Proceq equipment model Pundit lab+ connected to a computer and controlled by the software Pundit Link's wave form display, a pair of transducers and suitable coupling paste for shear wave readings, wave frequency of 250 kHz and a 25 μs calibration bar were used. Figure 5A and 5B show the calibration of the equipment and one of the tests being conducted, respectively.

Figure 5. Equipment for UPV measurements being (A) calibrated and (B) used in the specimens.

A numerical quantity called Recovery Factor (RF) was established to properly compare the results obtained by the UPV technique. The RF is found by applying Equation 1.

$$RF = \left[\frac{(UPV_{SFR} - UPV_{FIS})}{(UPV_{INT} - UPV_{FIS})}\right] x\ 1 \tag{1}$$

Where: UPV_{INT} is the ultrasonic pulse velocity for the intact specimen; UPV_{FIS} is the ultrasonic pulse velocity for the fissured specimen; UPV_{SFR} is the ultrasonic pulse velocity for the self-repaired specimen.

The denominator of Equation 1 gives the speed reduction of the ultrasonic pulse due to the induced fissures. The numerator provides the speed recovery of the ultrasonic pulse due to the admixture's self-healing activity. The division of these two values brings to light how effective the admixture was to self-heal each specimen. Note that the RF value is a percentage. So, a RF equal to 0% indicates inactivity of the proposed self-healing system. Otherwise, a RF equal to 100% suggests the total closure of the fissures.

2.6.2 Electrochemical impedance spectroscopy (EIS) tests

The assessment of the concrete self-healing ability through electrochemical testing consists of monitoring the development of the concrete's reinforcement corrosion when the concrete samples are intact and self-repaired. So, the closer the self-repaired corrosion results are of the intact corrosion results the greater is the concrete self-healing ability.

The EIS measurements were performed in two groups of prismatic specimens. The group A was formed by specimens that were not subjected to flexural tensile tests to induce fissures (intact specimens). Group B, on the other hand, was subjected to flexural tensile tests to induce fissures, left to rest during two days on environmental conditions, and then tested for corrosion. Table 2 shows the mentioned groups, as well as the test routines they were submitted.

Table 2 - Scheme for performing the tests according to the groups of specimens.

Groups	Specimens	Tests
A	3 Control	Electrochemical tests with intact specimens.
	3 ADT_3%	
	3 ADT_6%	
B	3 Control	Flexural tensile tests to cause fissures. 2 days of rest for self-healing action. Electrochemical tests after self-healing.
	3 ADT_3%	
	3 ADT_6%	

The flexural tensile tests performed to cause fissures and, consequently, stimulate the beginning of self-repairing process were conducted in a SHIMADZU servo-hydraulic universal testing machine, model UH – 2000kN XR, with appropriate support and force application devices. A linear displacement sensor (LVDT - Linear Variable Displacement Transducer) was used to monitor the strain of the specimen due to the application of loading and it was positioned with the aid of a yoke (LVDT sensor support). The ABNT NBR 12142 [29] was used as normative basis, and adaptations were made to a better fit with the research needs. The loading application rate was 0.9 MPa/min. The specimens were

positioned on the equipment with the longitudinal face, which contains the rebars, facing downwards and the two supports of the equipment were positioned 2.5cm from the vertical faces of the specimens. Figure 6 shows the apparatus assembled and ready to run a flexural tensile test.
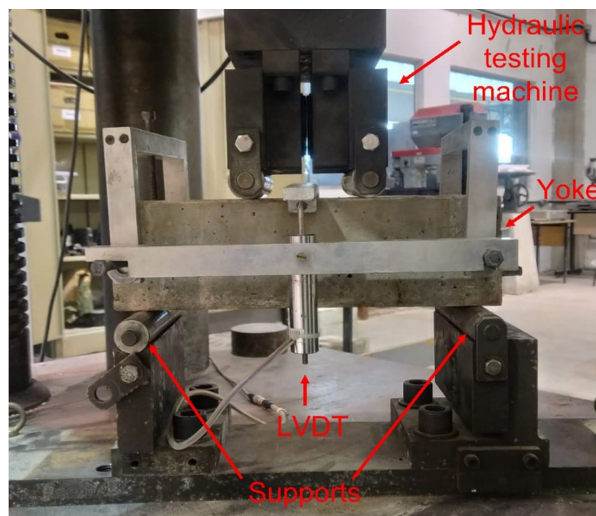

Figure 6. Prismatic specimen at the SHIMADZU universal testing machine ready to start the flexural test.

Before carrying the flexural tests for inducing fissures some considerations were done. First, the induced fissures must act as triggers for the self-repairing process. Second, they should be large enough to break the microcapsules and suitably small for being healed by the monomer available inside microcapsules. So, the strategy adopted was to conduct a flexural test in a sacrificial specimen until failure to observe the region of transition from the elastic to the plastic regime as it is when the first fissures initiate in the concrete. After carrying this test out, it was observed the displacement value indicated by the LVDT when the transition from the elastic to the plastic regime was reached. Then, it was decided to perform the tests on the other specimens up to a slightly higher value to ensure the fissures generation in all specimens. Similar procedures have been successfully used in other works [30]-[32].

The EIS analyses were performed using a Gamry Instruments potentiostat model Reference 600 controlled by the Gamry Framework software. The measurements were made at the open circuit potential. The parameters for carrying the EIS tests out were disturbance amplitude of 10mV rms, frequency range between 105 Hz and 10^{-2} Hz and 10 records per frequency logarithmic decade. The electrolyte used was a 5% NaCl by mass solution where the specimens were partially immersed. The tests lasted 55 days and measurements were taken every 5 days. The working electrode (WE) was one of the carbon steel rebars embedded in the specimens and the counter electrode (CE) was the 316L stainless steel rebar.

3 RESULTS AND DISCUSSIONS

3.1 Synthesized microcapsules characterization

The PUFM microcapsules containing the solution of MMA and DMPT 1% (mass of DMPT / mass of MMA) obtained according to the procedure described in Section 3.2 were characterized for morphology by scanning electron microscopy. Images A and B of Figure 7 show an overview and an approximated view of a representative sample of microcapsules, respectively.

The images revealed that the obtained microcapsules have a well-defined rounded shape with an average size distribution between 60μm and 120μm. In addition, it was observed no agglomeration tendency for the microcapsules, what makes their dispersion in concrete matrix easier.

To assess their size distribution, the microcapsules were evaluated by the laser diffraction method. The Figure 8 presents a histogram of volumetric distribution and a curve of accumulated values. In the histogram, two populations of microparticles can be seen (bimodal distribution), one of low and another of high volumetric intensity. The population with low volumetric intensity presents microcapsules with sizes between 6μm and 30μm while the one of high intensity is composed by microcapsules between 40μm and 110μm.
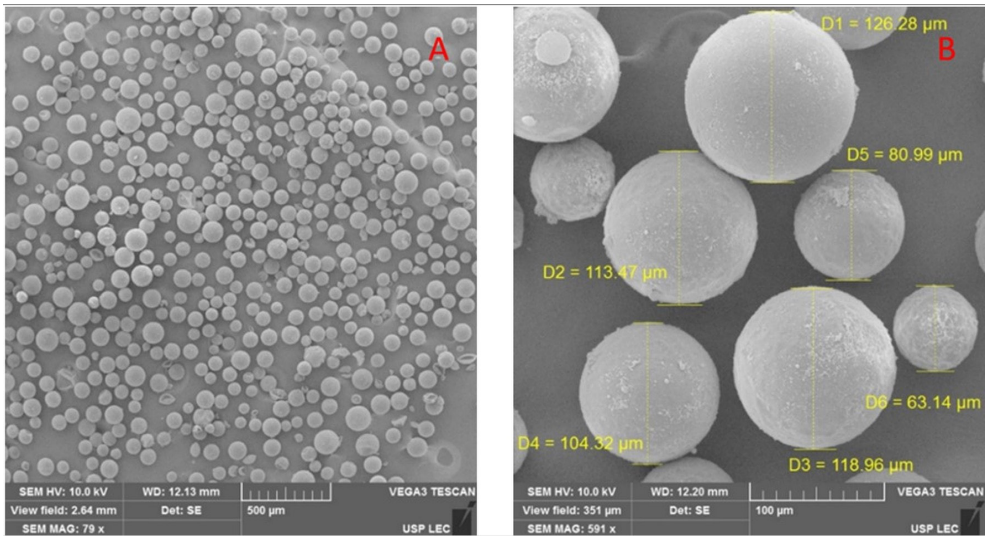
Figure 7. Images of microcapsules obtained by SEM: (A) Overview and (B) Approximate view with detail of measurements.
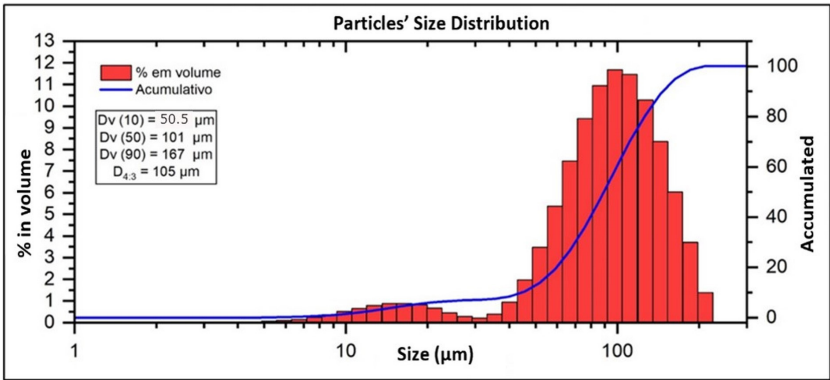

Figure 8. Volumetric distribution histogram and cumulative value curve of synthesized microcapsules.

The average volumetric diameter D (4,3) found using this technique was equal to 105μm. The volumetric diameters Dv (10), Dv (50), and Dv (90) showed that 10% of the sample's volume is composed of microcapsules with diameters up to 50.5μm, 50% of the sample's volume has diameters up to 101μm and 90% of the sample's volume has diameters up to 167μm, respectively. It is important to clarify that large microcapsules are positive in this case, as it means a higher availability of healing agent to fill up fissures.

Comparing the particles sizes indicated by SEM and laser diffraction analysis, it can be seen that a major part of microcapsules presents diameters from 60μm to 167μm. The dimensions of microcapsules obtained in this work are similar to those observed in other studies developed on the same topic [33], [34].

3.2 Influence of the self-healing system on concrete's characteristics

3.2.1 Water absorption

The water absorption test was carried out to verify whether the microcapsules' presence significantly changed the water ingress through the permeable voids of cementitious matrix. The tests followed the established by the American Society for Testing and Materials ASTM C0642 [35], and the results are shown in Table 3 and Table 4.

Observing the results shown in Table 3, the absorption values obtained for the three evaluated systems were quite similar. Aiming to verify whether there was any valid statistical difference among them, an ANOVA test with 95% of confidence was conducted using the software PAST, and its results are presented by Table 4.

Rev. IBRACON Estrut. Mater., vol. 17, no. 2, e17206, 2024

8/17

Table 3. Results of water absorption tests by immersion and boiling.

Specimen Identification (170 x 100 x 100) mm	m_s (g)	m_{sat} (g)	Absorption (%)	Standard deviation
Control 1	3343.86	3665.46		
Control 2	3314.65	3636.15	9.82	0.28
Control 3	3201.77	3526.45		
ADT_3 %_1	3229.88	3559.60		
ADT_3 %_2	3228.79	3555.84	10.36	0.33
ADT_3 %_3	3225.52	3571.77		
ADT_6 %_1	3203.89	3542.34		
ADT_6 %_2	3159.03	3492.91	10.55	0.03
ADT_6 %_3	3128.27	3457.15		

Table 4. Absorption ANOVA test results obtained with software PAST

	Sum of sqrs	df	Mean square	F value	p value
Between groups	0.858015	2	0.429008		
Within groups	0.37695	6	0.0628251	6.829	0.02844
Total	1.23497	8			

Analyzing the ANOVA results presented by Table 4, it was verified that the p value obtained was smaller than 0.05 (5%), what means there was at least a valid statistical difference among the absorption values compared. To identify which values were different from each other a Tukey test with 95% of confidence was carried out using the software PAST, and the results are presented by Table 5.

Table 5. Absorption Tukey test results obtained with software PAST

	Control	ADT_3%	ADT_6%
Control		p = 0.08656	p = 0.02756
ADT_3%	F = 3.719		p = 0.6408
ADT_6%	F = 5.04	F = 1.321	

As the Tukey test compares values two by two, it was possible to conclude analyzing Table 5 that only the comparison between the systems *Control* and ADT_6% presented a statistically valid difference with 95% of confidence.

Analyzing the water absorption results, it was possible to conclude that by adding 3% of microcapsules to the concrete matrix there was not significant impact in the concrete's water absorption property. Otherwise, the addition of microcapsules in a higher dosage (6%) caused a slightly increase in the concrete's porosity, what made the concrete more prone to the water permeation. A possible explanation to this is that when mixing a higher content of microcapsules (6%) into the fresh concrete, a significant quantity of microcapsules was prematurely broken what led to an unexpected release of healing agent. As the MMA has a certain level of volatility, part of it likely scaped from fresh concrete leaving some voids and making concrete more prone to water absorption. The same could have happened with the 3% addition but in a smaller scale what did not affect the concrete's tightness considerably.

3.2.2 Compressive Strength

The compressive strength tests were conducted according to the Brazilian National Standards Organization ABNT NBR 12142 [36] and the results are shown in Table 6.

Analyzing the results of Table 6 it was possible to see that the addition of the proposed self-healing admixture slightly increased the compressive strength of the concrete. To verify if the differences were statistically valid, an ANOVA testing at 95% of confidence was conducted with the three systems evaluated. The Table 7 exhibits the ANOVA results.

Table 6. Results of compressive strength tests.

Specimen Identification (cylindrical)	Compression Strength (MPa)	Average Compression Strength (MPa)	Standard deviation
Control 1	20.39		
Control 2	19.07		
Control 3	18.72	19.42	0.74
Control 4	20.02		
Control 5	18.90		
ADT_3%_1	19.09		
ADT_3%_2	20.86		
ADT_3%_3	21.41	20.67	0.93
ADT_3%_4	21.26		
ADT_3%_5	20.74		
ADT_6%_1	24.27		
ADT_6%_2	24.98		
ADT_6%_3	25.40	24.47	0.70
ADT_6%_4	23.99		
ADT_6%_5	23.71		

Table 7. Compressive strength ANOVA test results obtained with software PAST

	Sum of sqrs	df	Mean square	F value	p value
Between groups	68.838	2	34.419		
Within groups	7.22428	12	0.602023	57.17	7.341E-7
Total	76.0623	14			

Analyzing the ANOVA results presented by Table 7, it was verified that the p value obtained was smaller than 0.05 (5%), what means there was at least a valid statistical difference among the mean compressive strength values. To identify which values were different from each other, a Tukey test at 95% of confidence was carried out using the software PAST, and the results are presented by Table 8.

Table 8. Compressive strength Tukey test results obtained with software PAST

	Control	ADT_3%	ADT_6%
Control		p = 0.05917	p = 7.467E-7
ADT_3%	F = 3.637		p = 1.531E-5
ADT_6%	F = 14.53	F = 10.89	

By analyzing the results from Table 8 it was possible to get two conclusions. First, the systems *Control* and ADT_3% were not statistically different. It means that adding 3% of microcapsules (mass of microcapsules / mass of cement) into concrete caused no positive or negative effects to its compressive strength. In addition, it showed that besides the microcapsules work as voids in the concrete that can make it weaker, when they are added at low contents (3%) there is no detrimental effects to the concrete's compressive strength. Xu et al. [37] and Jiang et al. [38] reported similar results when adding microcapsules to the concrete at contents lower than 4% and between 1% and 3%, respectively. Second, the system ADT_6% is statistically different from the others i.e., by adding 6% of microcapsules to the concrete, its compressive strength increased around 25%. The raising of compressive strength can be explained by the presence of the APTES [39]-[41] on the microcapsules' shell. The hydrolyzed APTES has the ability of both delaying the cement hydration process by forming a layer on the surface of cement grains due to the presence of negative charges of the organic chain [42] and increasing the concrete's flexural and compressive strength. The mechanism behind the improvement of the concrete's mechanical properties is still not completely comprehended [39], [40], [43], [44]. Kong et al. [39] have reported improved flexural and compressive strength for mortar specimens containing APTES at 1% (mass of APTES / mass of cement). It was also interesting to note that the same effect was not observed for the samples containing only 3% of microcapsules. It could have happened due to the difference of quantity. The concrete samples containing more microcapsules consequently had more APTES what led to a more pronounced activity of this component.

Rev. IBRACON Estrut. Mater., vol. 17, no. 2, e17206, 2024

10/17

3.2.3 Indirect tensile strength

The results of the Brazilian test to indirectly verify the concrete's tensile strength are shown in Table 9.

Table 9. Results of tensile strength tests by diametral compression.

Specimen Identification (cylindrical)	Tensile Strength (MPa)	Average Tensile Strength (MPa)	Standard deviation
Control 6	1.78		
Control 7	1.91		
Control 8	2.63	1.96	0.38
Control 9	1.81		
Control 10	1.68		
ADT_3%_6	2.05		
ADT_3%_7	2.64		
ADT_3%_8	1.50	2.14	0.48
ADT_3%_9	1.92		
ADT_3%_10	2.58		
ADT_6%_6	2.39		
ADT_6%_7	2.62		
ADT_6%_8	1.74	2.32	0.40
ADT_6%_9	2.71		
ADT_6%_10	2.11		

Observing the results exposed by Table 10, it was possible to see that there was a sensible variation in the concrete's tensile strength due to the microcapsules addition. Aiming to reliably verify the existence of a valid statistical variation, it was conducted an ANOVA test at 95% of confidence.

Table 10. Tensile strength ANOVA test results obtained with software PAST

	Sum of sqrs	df	Mean square	F value	p value
Between groups	0.30976	2	0.15488		
Within groups	2.12168	12	0.176807	0.876	0.4415
Total	2.43144	14			

Analyzing the results presented by Table 10, it was possible to verify that the p value obtained in the ANOVA test was superior to 0.05 (5%) what means that there was not a statistical valid difference among the numbers compared. Despite that, observing the tensile strength mean values of the systems under evaluation, it was possible to note that as the microcapsules content increased the tensile strength also increased, vide Figure 9.
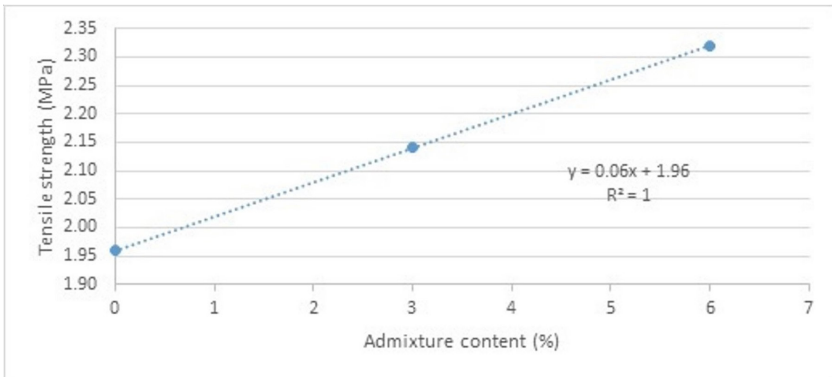

Figure 9. Correlation between tensile strength and admixture content

This behavior was also observed in the compressive strength results. Thus, such trend can also be related to the previous commented presence of APTES. In addition, confronting compression, and tensile strength results, it was possible to verify, for all systems under investigation, that the tensile strength values represented around 10% of their respective compressive strength result, as it can be seen in Table 11. This fact showed that the tensile strength values increased proportionally to the compression strength.

Table 11. Comparison between average values of compression and tensile strength results

System Identification (cylindrical)	Average Compression Strength (MPa)	Average Tensile Strength (MPa)	Ratio
Control	19.42	1.96	10.1 %
ADT_3 %	20.67	2.14	10.4 %
ADT_6 %	24.47	2.32	9.5 %

3.3 Evaluation of the self-repair of concrete

3.3.1. Assessment of self-repair by ultrasonic pulse velocity tests

The UPV tests were carried out to access the efficiency of the proposed self-healing system, and the results are presented by Table 12.

Table 12. UPV test results

Specimen Identification	Ultrasonic wave speed (m/s)		
	Intact	Fissured	Self-repaired
CONTROL_1	4112.70	4030.12	4062.75
CONTROL_2	4038.93	3957.83	3957.83
CONTROL_3	4165.98	3924.71	3924.71
ADT_3 %_1	3795.45	3670.33	3738.81
ADT_3 %_2	3891.89	3200.21	3549.30
ADT_3 %_3	4046.18	3547.54	3677.01
ADT_6 %_1	3868.73	3540.64	3591.40
ADT_6 %_2	3791.67	3653.28	3763.16
ADT_6 %_3	3864.86	3600.72	3653.28

It is important to mention that the three systems under assessment presented one sample behaving differently from the others i.e., Control_1, ADT_3%_3 and ADT_6%_2. Thus, for discussion purposes they were considered as outliers, but their numerical contributions were included in the recovery factor calculations once they did not change the overall conclusions.

Analyzing the *Control* system data exposed by Table 12 and Figure 10, it was possible to note that the highest values were verified when the three specimens were intact, as expected. On the other hand, after inducing the fissures by applying 80% of concrete samples' ultimate compressive strength load, a drop in the waves speed was observed (vide Fissured column in Table 12). Such decreasing on speed is explained by the presence of fissures which worked as discontinuities in the concrete matrix, hindering the waves' travel through the samples. Analyzing the results of the specimens CONTROL_2 and CONTROL_3, two days after the compression tests (vide Self-repaired column in Table 12), it was possible to verify that there was not variation in the speed of the waves when comparing them with the fissured situation. This fact showed that the control specimens did not present self-healing ability, as expected. The sample CONTROL_1 presented a different behavior. It can be explained by the heterogeneity of the concrete mentioned by other authors as an obstacle to the good reproducibility of the tests performed on concrete [45], associated with some variation in the positioning of the transducers between one reading and another. Despite this, the set of results leads to the conclusion that there was no self-repairing of the *Control* specimens.
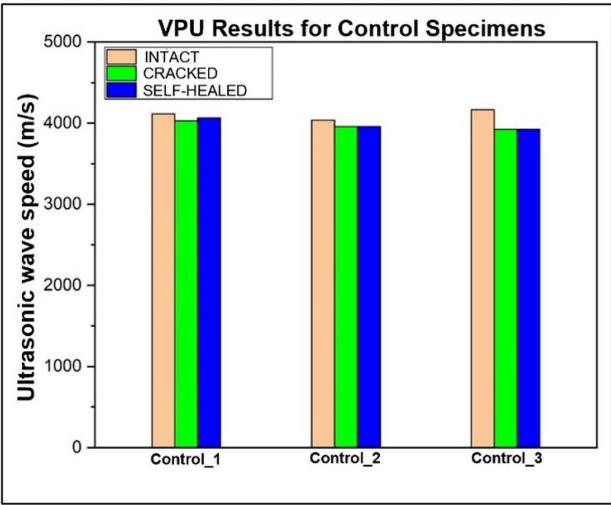
Rev. IBRACON Estrut. Mater., vol. 17, no. 2, e17206, 2024

12/17

Figure 10. UPV results obtained for specimens with no admixtures (*Control*).

The results obtained for the specimens with 3% of addition are shown in Figure 11 and Table 12. The highest values of ultrasonic wave speed were obtained for the intact condition, followed by the self-repaired and fissured. The higher speeds obtained for the self-repaired condition in comparison to the fissured state showed that a self-repairing activity took place. However, the fissures were not completely sealed. This affirmation was made based on the difference observed between the values of the intact and self-repaired conditions. Once they were not equal, the wave speed recovery was not total.
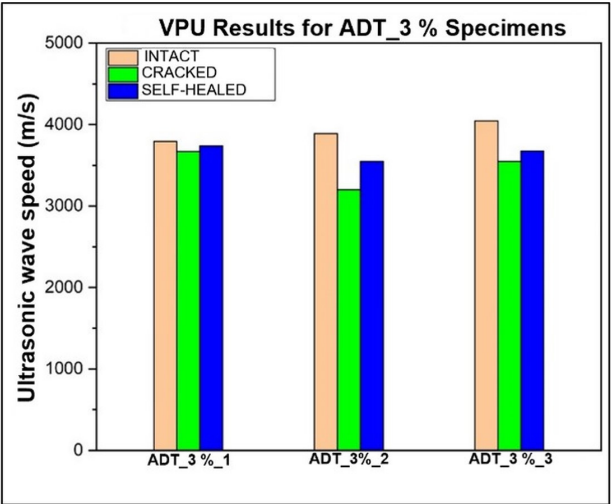

Figure 11. UPV results obtained for specimens with 3 % addition.

The ADT_6% system results are exposed in Figure 12 and Table 12. Analyzing this data set, it was also possible to verify self-repairing activity. However, the damage recovery was less pronounced than the one observed for the ADT_3 % system. This result could also be associate to the possible rupture of capsules during the mixing process which had reduced the effectiveness of self-healing system.

To establish clearer comparison among results, the Table 13 shows the recovery factor (RF) values obtained through the application of Equation 1.

The average RF obtained for the system ADT_3% was 44%. It reinforced the conclusion that the samples of this system had their fissures partially sealed. On the other hand, two of the three specimens of the system ADT_6% presented low recovery factor values. This poor performance can be related to the potentially high quantity of microcapsules broken during the mixing process.
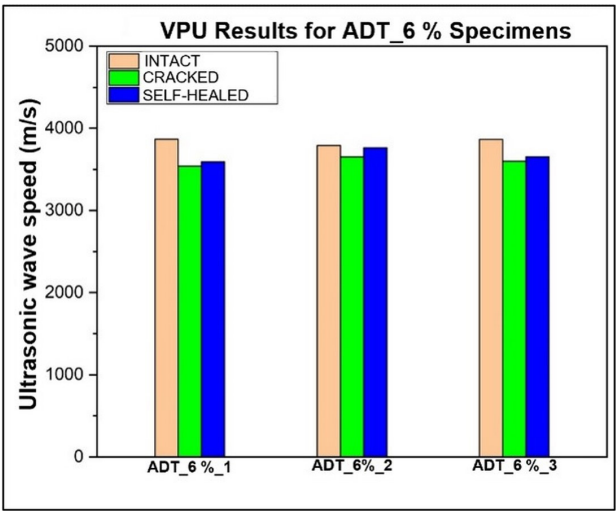
Figure 12. UPV results obtained for specimens with 6 % addition.

Table 13. RF values obtained with the UPV technique

Specimen Identification	Recovery Factor (%)	Average value (%)
ADT_3%_1	54.73	
ADT_3%_2	50.48	44
ADT_3%_3	25.96	
ADT_6%_1	15.47	
ADT_6%_2	79.40	38
ADT_6%_3	19.90	

3.3.2. Assessment of self-repair by EIS tests

After approximately 28 days of cure in a humidity chamber, the reinforced prismatic specimens were subjected to the Electrochemical Impedance Spectroscopy tests. The EIS trials took 55 days, and the readings were taken every 5 days. During the entire evaluation period, the specimens were partially immersed in a 5 % by mass NaCl solution.

The EIS results obtained for the three systems in the INTACT condition were plotted in a diagram that shows the progression of impedance modulus ($|Z|$) at a frequency of 10^{-2} Hz over the time (Figure 13). The option for analyzing the $|Z|$ at low frequencies was made because, in this way, it was possible to observe the reinforcement's electrochemical behavior. It is important to point out that higher impedance modulus at low frequencies (LF) means better corrosion resistance of the embedded carbon steel rebars (reinforcements).
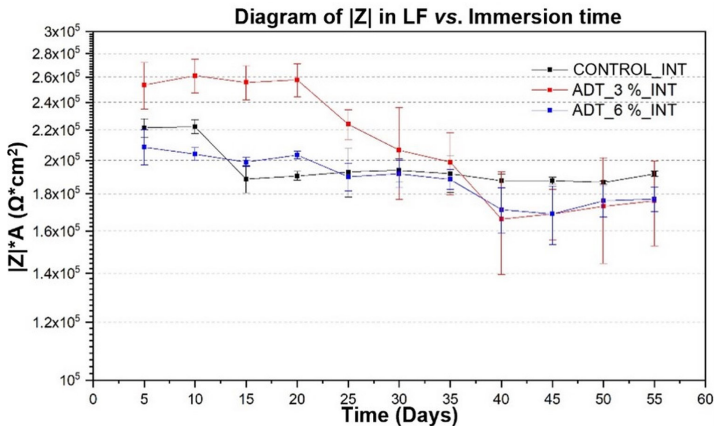

Figure 13. EIS results of the three systems evaluated in the INTACT condition.

Rev. IBRACON Estrut. Mater., vol. 17, no. 2, e17206, 2024

14/17

Analyzing Figure 13, it was possible to verify that in the INTACT condition the group ADT_3% presented mean values of |Z| higher than the other groups during the first 25 days. Furthermore, this group did not present a downward trend up to 20 days. It means that during this period, the ADT_ 3% concrete specimens were less susceptible to reinforcement corrosion. However, after this time a gradual decreasing of |Z| was observed, and. after 30 days this group reached its lowest value (numerical equal to the |Z| values of the other groups). On the other hand, the curves referring to the systems *Control* and ADT_6% showed very similar behavior during the whole immersion time. It led to the conclusion that the presence of microcapsules did not negatively impact the concrete's barrier property. This fact is reinforced by the results of the groups containing 3% and 6% of microcapsules which were or better or similar to the results of the group *Control*.

The Figure 14 shows the EIS results for specimens in the REPAIRED condition. The analysis of this diagram showed that the *Control* system presented a downward trend since the beginning of the test. The ADT_6% group also presented a decrease in the values of |Z| over time. However, the ADT_6%'s rate of decrease was less pronounced than the control's one. From the measurements taken at (40, 45 and 55) days, it was possible to verify a better performance of ADT_6% in comparison to the *Control* system.
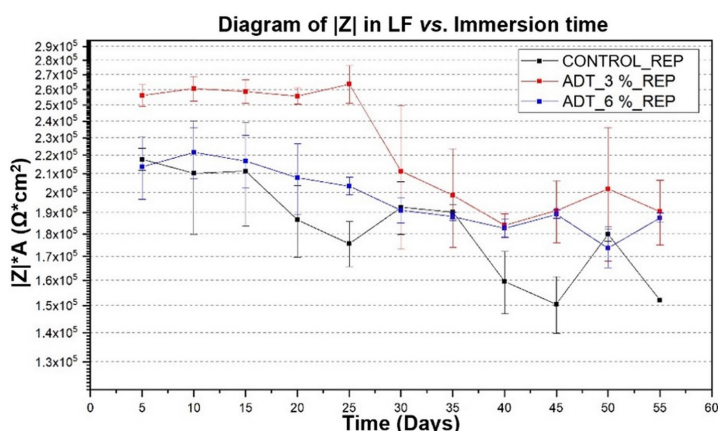

Figure 14. EIS results of the three systems evaluated in the REPAIRED condition.

The results of the ADT_3% group presented in Figure 14, showed that this system presented the best electrochemical performance among the other groups during the first 25 days of immersion for the REPAIRED condition. Furthermore, it is important to mention that the performances of this system in the INTACT and REPAIRED conditions were very similar, showing that there may have been self-repairing. Another relevant point is that the ultrasound tests showed good self-repairing activity for this system, with recovery factors (RF) above 50 % for two of the three specimens of the triplicate. This fact supports the conclusion that this system presented repairing activity.

5 CONCLUSIONS

Through SEM analysis, it was possible to verify that the microcapsules presented a regular, well-defined spherical shape and sizes varying between 60μm and 120 μm. Through the laser diffraction technique, it was possible to verify that the microcapsules presented a size distribution between 50.5μm and 167μm and an average diameter of 105μm.

The addition of microcapsules into the concrete at 3% regarding the cement mass did not impact its compressive strength. On the other hand, the addition of microcapsules at 6% positively influenced this characteristic, causing a remarkable improvement to this property (around 25%). Furthermore, it was verified a consistent relation between the microcapsules content and the tensile strength i.e., the higher the microcapsules content the greater the tensile strength.

The water absorption tests showed that the addition of 3% of microcapsules did not change the watertightness of the concrete. Regarding the 6% addition, an increase of about 7% was observed in the concrete's water absorption. Thus, it was concluded that the microcapsules content can influence the concrete's watertightness.

The UPV and EIS tests carried out to verify self-repairing activity showed that the admixture were able to heal the concrete's fissures partially. In addition, analyzing the recovery factor values (RF) obtained for these two systems, it was concluded that the samples with 3% of microcapsules presented higher self-repairing rates.

Despite the microcapsules developed in this work have presented a satisfactory self-healing efficiency, their effectiveness looks to be affected by the mixing procedure once part of them is broken during the process. Thus, a good suggestion for future works would be make the microcapsules' shell less susceptible to the concrete's mixing process.

The results presented on this article showed that nondestructive tests as UPV and EIS are techniques sufficiently sensible to investigate self-healing activities on concrete.

ACKNOWLEDGEMENTS

REFERENCES

[1]   S. R. White et al., "Autonomic healing of polymer composites," *Nature*, vol. 409, pp. 794–797, 2001.

[2]   C. Edvardsen, "Water permeability and autogenous healing of cracks in concrete," *Mater. J.*, vol. 96, no. 4, pp. 448–454, Jul 1999.

[3]   M. Roig-Flores and P. Serna, "Concrete early-age crack closing by autogenous healing," *Sustainability*, vol. 12, no. 11, pp. 4476, Jun 2020.

[4]   M. R. De Rooij et al., *Self-healing phenomena in cement-based materials*. Dordrecht: Springer, 2013.

[5]   M. Rajczakowska et al., "Autogenous self-healing: a better solution for concrete," *J. Mater. Civ. Eng.*, vol. 31, no. 9, pp. 03119001, Jun 2019.

[6]   A. Sidiq, R. Gravina, and F. Giustozzi, "Is concrete healing really efficient? A review," *Constr. Build. Mater.*, vol. 205, pp. 257–273, Apr 2019.

[7]   K. Van Tittelboom and N. De Belie, "Autogenous healing of cracks in cementitious materials with varying mix compositions", in *2nd International conference Self-Healing Materials*, 28 jun. 2009.

[8]   K. Zhenga, X. Yang, R. Chen, and L. Xu, "Application of a capillary crystalline material to enhance cement grout for sealing tunnel leakage," *Constr. Build. Mater.*, vol. 214, pp. 497–505, 2019.

[9]   C. Britez et al., "Estanqueidade de lajes de subpressão: caso MIS-RJ," in: *55 Congresso Brasileiro de Concreto*, 2013.

[10] I. R. Almeida, "A onda de concreto que flutua no M.A.R.," *Rev. Concr. Constru.*, vol. 72, pp. 100–110, Oct/Dec 2013. Accessed: Apr. 25, 2023. [Online]. Available: http://ibracon.org.br/Site_revista/Concreto_Construcoes/pdfs/capa72.pdf

[11] P. Giannaros, A. Kanellopoulos, and A. Al-Tabbaa, "Sealing of cracks in cement using microencapsulated sodium silicate," *Smart Mater. Struct.*, vol. 25, no. 8, 2016.

[12] J. Gilford et al., "Dicyclopentadiene and sodium silicate microencapsulation for self-healing of concrete," *J. Mater. Civ. Eng.*, vol. 26, no. 5, pp. 886–896, 2014.

[13] H. M. Jonkers, "Self healing concrete: a biological approach," *Springer Ser. Mater. Sci.*, vol. 100, pp. 195–204, 2007.

[14] J. Milla, M. M. Hassan, and T. Rupnow, "Evaluation of self-healing concrete with microencapsulated calcium nitrate," *J. Mater. Civ. Eng.*, vol. 29, no. 12, pp. 04017235, 2017.

[15] H. M. Jonkers et al., "Application of bacteria as self-healing agent for the development of sustainable concrete," *Ecol. Eng.*, vol. 36, no. 2, pp. 230–235, Feb 2010.

[16] N. P. B. Tan et al., "Silica-based self-healing microcapsules for self-repair in concrete," *J. Appl. Polym. Sci.*, vol. 133, no. 12, pp. 43090, Mar 2016.

[17] Z. Yang et al., "Laboratory assessment of a self-healing cementitious composite," *Transp. Res. Rec.*, vol. 2142, no. 2142, pp. 9–17, Jan 2010.

[18] I. Aoki and F. Cotting, "Coating self-healing effect by loading microcapsules with two-component epoxy film former," in: EuroCorr, 2014

[19] F. Cotting, A. Koebsch, and I. V. Aoki, "Epoxy self-healing coating by encapsulated epoxy ester resin in poly (urea-formaldehyde-melamine) microcapsules," *Front. Mater.*, vol. 6, pp. 5, Dec 2019.

[20] Associação Brasileira de Normas Técnicas, *Concreto - Procedimento para Moldagem e Cura de Corpos de Prova*, NBR 5738, 2015.

[21] Associação Brasileira de Normas Técnicas, *Argamassa e Concreto Endurecidos - Determinação da Absorção de Água, índice de vazios e massa específica*, NBR 9778, 2005.

[22] Associação Brasileira de Normas Técnicas, *Concreto - Ensaio de Compressão de Corpos de Prova Cilíndricos*, NBR 5739, 2018.

[23] Associação Brasileira de Normas Técnicas, *Concreto e Argamassa — Determinação da Resistência à Tração por Compressão diametral de Corpos de Prova Cilíndricos,* NBR 7222, 2011.

[24] L. A. Camara et al., "Monitoring the self-healing of concrete from the ultrasonic pulse velocity," *J. Compos. Sci.*, vol. 3, no. 1, pp. 1, Mar 2019.

[25] A. Lorenzi et al., "Avaliação da capacidade de detecção de falhas no concreto através do ensaio ultrassônico," *Rev. ALCONPAT*, vol. 7, no. 3, pp. 286–301, Sep 2017.

[26] R. H. Geraldo, A. M. Guadagnini, and G. Camarini, "Self-healing concrete with crystalline admixture made with different cement content," *Ceramica*, vol. 67, no. 383, pp. 370–377, Sep 2021.

[27] Z. Yang et al., "A self-healing cementitious composite using oil core/silica gel shell microcapsules," *Cement Concr. Compos.*, vol. 33, no. 4, pp. 506–512, Apr 2011.

[28] Associação Brasileira de Normas Técnicas, *Concreto endurecido - Determinação da Velocidade de Propagação de Onda Ultrassônica*, NBR 8802, 2019.

[29] Associação Brasileira de Normas Técnicas, *Concreto - Determinação da Resistência à Tração na Flexão de Corpos de Prova Prismáticos*, NBR 12142, 2010.

[30] L. Ferrara, V. Krelani, and M. Carsana, "A "fracture testing" based approach to assess crack healing of concrete with and without crystalline admixtures," *Constr. Build. Mater.*, vol. 15, Oct 2014, http://dx.doi.org/10.1016/J.CONBUILDMAT.2014.07.008.

[31] S. Granger, A. Loukili, G. Pijaudier-Cabot, and G. Chanvillard, "Experimental characterization of the self-healing of cracks in an ultra high performance cementitious material: Mechanical tests and acoustic emission analysis," *Cement Concr. Res.*, vol. 37, no. 4, pp. 519–527, Apr 2007, http://dx.doi.org/10.1016/j.cemconres.2006.12.005.

[32] E. Mostavi, S. Asadi, M. M. Hassan, and M. S. Alansari, "Evaluation of self-healing mechanisms in concrete with double-walled sodium silicate microcapsules," *J. Mater. Civ. Eng.*, vol. 27, no. 12, pp. 04015035, Oct 2015, http://dx.doi.org/10.1061/(ASCE)MT.1943-5533.0001314.

[33] B. Dong, N. Han, M. Zhang, X. Wang, H. Cui, and F. Xing, "A microcapsule technology based self-healing system for concrete structures," *J. Earthq. Tsunami*, vol. 26, Nov 2013, http://dx.doi.org/10.1142/S1793431113500140.

[34] N. P. B. Tan et al., "Silica-based self-healing microcapsules for self-repair in concrete," *J. Appl. Polym. Sci.*, vol. 133, no. 12, pp. 43090, Mar 2016.

[35] American Society for Testing Materials, *Standard Test Method for Density, Absorption, and Voids in Hardened Concrete*, ASTM C0642, 2021.

[36] Associação Brasileira de Normas Técnicas, *Concreto - Determinação da Resistência à Tração na Flexão de Corpos de Prova Prismáticos*, NBR 12142, 2010.

[37] N. Xu et al., "Employing ultrasonic wave as a novel trigger of microcapsule self-healing cementitious materials," *Cem Concr Compos*, vol. 118, pp. 103951, Apr 2021.

[38] S. Jiang et al., "Preparation and mechanical properties of microcapsule-based self-healing cementitious composites," *Materials (Basel)*, vol. 14, no. 17, pp. 4866, Aug 2021.

[39] X. Kong, H. Liu, Z. Lu, and D. Wang, "The influence of silanes on hydration and strength development of cementitious systems," *Cement Concr. Res.*, vol. 67, pp. 168–178, 2015, http://dx.doi.org/10.1016/j.cemconres.2014.10.008.

[40] F. Svegl, J. Suput-Strupi, L. Skrlep, and K. Kalcher, "The influence of aminosilanes on macroscopic properties of cement paste," *Cement Concr. Res.*, vol. 2008, no. 38, pp. 945–954, Feb 2008, http://dx.doi.org/10.1016/j.cemconres.

[41] A. Pop, A. Bede, M. C. Dudescu, F. Popa, and I. Ardelean, "Monitoring the influence of aminosilane on cement hydration via low-field NMR relaxometry," *Appl. Magn. Reson.*, vol. 47, pp. 191–199, Nov 2015, http://dx.doi.org/10.1007/s00723-015-0743-7.

[42] A. Cretu, C. Mattea, S. Siegfried, and I. Ardelean, "The effect of silica fume and organosilane addition on the porosity of cement paste," *Molecules*, vol. 25, no. 8, pp. 1762, Apr 2020, http://dx.doi.org/10.3390/molecules25081762.

[43] J. Milla et al., "Effect of self-healing calcium nitrate microcapsules on concrete properties," *Transp. Res. Rec. J. Transp. Res.*, vol. 2577, pp. 69–77, 2016.

[44] X. Wang et al., "Laboratory and field study on the performance of microcapsule-based self-healing concrete in tunnel engineering," *Constr. Build. Mater.*, vol. 220, pp. 90–101, Sep 2019.

[45] P. Romano, P. S. D. Brito, and L. Rodrigues, "Monitoring of the degradation of concrete structures in environments containing chloride ions," *Constr. Build. Mater.*, vol. 47, pp. 827–832, Oct 2013.